Exploring the canonical behaviour of long Gamma-Ray Bursts using an intrinsic multi-wavelength afterglow correlation

S. R. Oates[a,*], J. L. Racusin[b], M. De Pasquale[c], D. Kocevski[d], M. J. Page[e], A. J. Castro-Tirado[f,g], J. Gorosabel[g,h,i,†], A. A. Breeveld[e], N. P. M. Kuin[e] and P. J. Smith[e]

[a] *School of Physics and Astronomy & Institute for Gravitational Wave Astronomy, University of Birmingham, B15 2TT, UK*

[b] *Astrophysics Science Division, NASA Goddard Space Flight Center, 8800 Greenbelt Road, Greenbelt, Maryland 20771, USA*

[c] *Dipartimento di Scienze Matematiche e Informatiche, Scienze Fisiche e Scienze della Terra (MIFT), Universitá di Messina - Viale F. Stagno d'Alcontres, 31 - 98166 Messina, Italy*

[d] *NASA Marshall Space Flight Center, Huntsville, AL*

[e] *Mullard Space Science Laboratory, University College London, Holmbury St. Mary, Dorking, Surrey, RH5 6NT, UK*

[f] *Instituto de Astrofísica de Andalucía (IAA-CSIC), Glorieta de la Astronomía s/n, E-18008, Granada, Spain*

[g] *Unidad Asociada Departamento de Ingeniería de Sistemas y Automática, E.T.S. de Ingenieros Industriales, Universidad de Málaga, Spain*

[h] *Unidad Asociada Grupo Ciencias Planetarias UPV/EHU-IAA/CSIC, Departamento de Física Aplicada I, E.T.S.*

[i] *Ingeniería, Universidad del País Vasco UPV/EHU, Bilbao, Spain*

[†] *deceased*

[*] *E-mail: s.r.oates@bham.ac.uk*

In this conference proceeding we summarise our investigation of a correlation discovered between the afterglow luminosity (measured at restframe 200 s; log L_{200s}) and average afterglow decay rate (measured from restframe 200 s onwards; $\alpha_{>200s}$) of long duration Gamma-ray Burst (GRB) afterglows, found in both the optical/UV and X-ray afterglows. We examine the correlation in the X-ray light curves and find that it does not depend on the presence of specific features in the X-ray light curve. We test how the optical and X-ray parameters log $L_{O,200s}$, log $L_{X,200s}$, $\alpha_{O,>200s}$, $\alpha_{X,>200s}$ relate to each other and to parameters from the prompt emission phase. Using a Monte Carlo simulation, we explore whether these relationships are consistent with predictions of a basic standard afterglow model. We conclude that most of the correlations we observe are consistent with a common underlying physical mechanism producing GRBs and their afterglows regardless of their detailed temporal behaviour, but this basic model has difficulty explaining correlations involving $\alpha_{>200s}$. We therefore briefly discuss alternative more complex afterglow models.

Keywords: Gamma-ray bursts; correlations

1. Introduction

Gamma-ray bursts (GRBs) are intense flashes of gamma-rays that are usually accompanied by an afterglow, longer lived emission that may be detected at X-ray to radio wavelengths. Studies of single GRBs provide exceptional detail on the behaviour and physical properties of individual events. However, statistical investigations of large samples of GRBs aim to find common characteristics and correlations

that link individual events and therefore provide insight into the mechanisms common to GRBs. Statistical investigations performed so far have found a number of trends and correlations within and linking the prompt gamma-ray emission and the afterglow emission e.g., Ref. 1–10.

In this conference proceeding, we focus on the discovery of a correlation, found in a sample of optical/UV afterglow light curves,[11] between the logarithmic brightness ($\log L_{O,200s}$; measured at restframe 200 s and at a restframe wavelength 1600 Å), and their average decay rate ($\alpha_{>200s}$; measured from restframe 200 s onwards with a single power-law). This correlation has also been found at X-ray wavelengths.[12] To gain insight into the origin of the luminosity-decay correlation, we investigated the X-ray sample and how it relates to other GRB properties.[12,13] Ref. 12 discovered the $\log L_{200s} - \alpha_{>200s}$ in the X-ray afterglows observed by the *Swift* X-ray Telescope (XRT[14]). Ref. 13 compared the parameters of the optical/UV $\log L_{200s} - \alpha_{>200s}$ correlation with the equivalent values from the X-ray and also explored their relationship to properties of the prompt emission, namely the isotropic energy E_{iso} and the peak energy E_{peak}. In the following, we will provide a summary of these papers.

2. Sample Selection

The X-ray light curves were retrieved from the University of Leicester *Swift*-XRT Team GRB repository.[15,16] Ref. 12 selected X-ray afterglows of *Swift*/BAT detected GRBs, that were observed between December 2004 and March 2014, that had measured redshifts, had at least 3 light curve bins and started within a factor of restframe 200 s, t_{200s}. The final sample includes 246 GRBs; 237 long and 9 short. The count rate light curves were converted to flux density at 1 keV using the spectral index from the automated fits to the photon counting mode data, and then to intrinsic luminosity. All light curve fitting is performed in the count rate domain.

The Ref. 13 sample, used to compare the properties of the X-ray, optical afterglows together with their prompt emission parameters, consists of 48 long GRBs that overlap the Ref. 11 and Ref. 12 samples. The optical/UV luminosity light curves were produced at a common wavelength of 1600 Å.[11]

To measure luminosity at 200 s, $\log L_{200s}$, for the optical/UV light curves we interpolated between 100 and 2000 s and for the X-ray we measured the luminosity at 200 s from the best-fit light curve model.[17] To obtain the average decay rate $\alpha_{>200s}$, a single power-law was fit to each optical/UV and X-ray light curve from 200 s onwards.

For some X-ray afterglows, an initial steep decay, associated with the tail of the prompt emission,[18] can contaminate the initial part of the X-ray light curve. Of the 246 X-ray light curves, the steep decay segment is found to contaminate 23 X-ray light curves at restframe 200 s. We identify a light curve segment to have a prompt origin if there is a steep to shallow transition with $\Delta\alpha > 1.0$. In these situations the average decay index is measured with a simple power-law fit to data beyond restframe 200 s and after the steep to shallow transition. In order to get a better

estimate of the afterglow luminosity at restframe 200 s, we extrapolate back to restframe 200 s the first segment of the best-fit light curve that is not contaminated by the prompt emission (see also Ref. 12).

To compare the afterglow properties with the prompt emission properties we determined the isotropic energy E_{iso} and restframe peak energy, E_{peak} from the γ-ray emission, following Ref. 17. Of the 48 GRBs that overlap the optical and X-ray samples,[11,12] we determined E_{peak} for 44 GRBs and E_{iso} for 47 GRBs.

We determine the strength of the correlation using the IDL tool *r_correlate*, which measures the Spearman rank coefficient (R_{sp}), and its corresponding null hypothesis probability (p). We also use the partial Spearman rank correlation to test the dependence of each correlation on redshift.

We perform a linear regression analysis using the IDL routines *fitexy* and *sixlin*: *fitexy* is used when both parameters have errors, *sixlin* is used when we do not know the errors on one or both parameters. Since there are only a handful of GRBs with errors on the E_{iso} and E_{peak} parameters, we choose to discard errors in both parameters and use *sixlin* when determining the strength and significance of each correlation with one of these parameters involved.

3. Results

3.1. $\log L_{X,200s} - \alpha_{X,>200s}$ *correlation*

Within the sample of 246 X-ray afterglow light curves we see evidence for a correlation between $\log L_{X,200s}$ and $\alpha_{X,>200s}$, similar to that in the optical/UV.[11] The X-ray afterglow sample consists of long and short GRBs and the light curves are often more complex than the optical/UV, consisting of features such as plateaus and flares that may add scatter or influence the correlation. We test these effects by dividing the sample by specific characteristics and reproducing the same analyses. We report all of these tests and the final correlation in Table 1 and Fig. 1.

The first test is to determine if the $\log L_{X,200s} - \alpha_{X,>200s}$ correlation is observed for both short and long GRBs. Separating GRBs in to long and short classes, we find that long GRBs are significantly correlated, but no significant correlation is found for the short GRBs. This suggests that their is some intrinsic difference in the afterglow properties of short and long GRBs, be it their environment or jet dynamics. For all further tests of the $\log L_{X,200s} - \alpha_{X,>200s}$ correlation, we exclude short GRBs.

X-ray flares have been shown to have an internal rather than external shock origin and may be a potential source of contamination in measuring the $\log L_{X,200s}$ and $\alpha_{X,>200s}$ parameters. We first separate those afterglows with X-ray flares (without removing flaring intervals) and those without flares, and find that the two samples show very similar correlation strengths and slopes, but with slightly more scatter in the sample with flares. We do not exclude GRBs with flares, instead we exclude the flaring intervals from the light curves and refit them to obtain $\log L_{X,200s}$ and

$\alpha_{\rm X,avg,>200s}$. Re-running the Spearman rank test, on the entire sample we find a tighter correlation. Henceforth, we therefore, continue our investigation using the flare-removed average decay fits.

The average decay rate may also be influenced by the plateau phase observed in some X-ray afterglows (e.g Ref. 17). For example, a light curve with an extremely long plateau (e.g. GRB 060729; Ref. 19) may have a shallower average decay, whereas GRBs without plateaus would be steeper. In addition Refs. 20, 21 have shown that there is a relationship between the time and flux of the end of the X-ray plateau, which could be another manifestation of the log $\rm L_{200s} - \alpha_{>200s}$ correlation. We thus divide the X-ray sample in to those with and without plateaus and to determine if the correlation is still present in both sub-samples. The results in Table 1 indicate that the luminosity-average decay correlation is present and similarly significant in both sub-samples. This suggests that the plateau feature is not responsible for producing the correlation and is not solely responsible for regulating the average afterglow decay.

Table 1. Linear regression and correlation statistics for each test of the X-ray light curve sample. The partial Spearman rank coefficient tests the dependence of the given set of parameters on redshift. For the regular or partial Spearman rank coefficient, the corresponding null hypothesis is given to its right. This table is adapted from Table 2 in Ref. 12.

Sample	Parameters		Spearman	Null	Partial	Null	Best fit linear regression		Number
	x-axis	y-axis	Rank	Hypothesis	Spearman Rank	Hypothesis	Slope	Constant	in Sample
Short	log $\rm L_{X,200s}$	$\alpha_{X,>200s}$	-0.07	> 0.10	0.11	> 0.10	$0.16^{+0.10}_{-0.39}$	$-3.40^{+11.16}_{-2.77}$	9
Long	log $\rm L_{X,200s}$	$\alpha_{X,>200s}$	0.59	$\ll 10^{-6}$	0.59	$\ll 10^{-6}$	$0.27^{+0.04}_{-0.04}$	$-6.99^{+1.23}_{-1.10}$	237
Flares	log $\rm L_{X,200s}$	$\alpha_{X,>200s}$	0.58	$\ll 10^{-6}$	0.56	$\ll 10^{-6}$	$0.30^{+0.07}_{-0.06}$	$-7.91^{+1.84}_{-2.17}$	134
No Flares	log $\rm L_{X,200s}$	$\alpha_{X,>200s}$	0.59	$\ll 10^{-6}$	0.64	$\ll 10^{-6}$	$0.28^{+0.03}_{-0.04}$	$-7.27^{+1.28}_{-1.01}$	103
Plateau	log $\rm L_{X,200s}$	$\alpha_{X,>200s}$	0.58	$\ll 10^{-6}$	0.55	$\ll 10^{-6}$	$0.26^{+0.05}_{-0.06}$	$-6.81^{+1.84}_{-1.43}$	156
No Plateau	log $\rm L_{X,200s}$	$\alpha_{X,>200s}$	0.57	$\ll 10^{-6}$	0.61	$\ll 10^{-6}$	$0.26^{+0.06}_{-0.05}$	$-6.82^{+1.60}_{-1.83}$	81
Final	log $\rm L_{X,200s}$	$\alpha_{X,>200s}$	0.59	$\ll 10^{-6}$	0.59	$\ll 10^{-6}$	$0.27^{+0.04}_{-0.04}$	$-6.99^{+1.23}_{-1.11}$	237

3.2. *Prompt emission and afterglow parameter comparison*

We now compare the parameters of the optical/UV and X-ray log $\rm L_{200s} - \alpha_{>200s}$ correlations using the 48 GRBs that overlap both samples. The results are given in Table 2. Using the same GRBs for the optical and X-ray log $\rm L_{200s} - \alpha_{>200s}$ correlation we find the slopes of the linear regressions are consistent at 1σ. When swapping the X-ray and optical/UV luminosity and decay parameters, i.e log $\rm L_{O,200s}$ versus $\alpha_{\rm X,>200s}$ and log $\rm L_{X,200s}$ versus $\alpha_{\rm O,>200s}$ we find similar strength relationships. Strong correlations are also observed when correlating log $\rm L_{O,200s}$ vs log $\rm L_{X,200s}$ and $\alpha_{\rm O>200s}$ vs $\alpha_{\rm X,>200s}$.

In Table 2 we also provide the results of the comparison of the parameters of the optical/UV and X-ray luminosity-decay correlations with the prompt emission parameters: log $\rm E_{iso}$ and $\rm E_{peak}$. Comparison of the optical/UV and X-ray luminosity with log $\rm E_{iso}$ indicates strong correlations and the slope of the linear regressions are consistent to within 1σ. We also provide the results of the comparison of log $\rm E_{iso}$

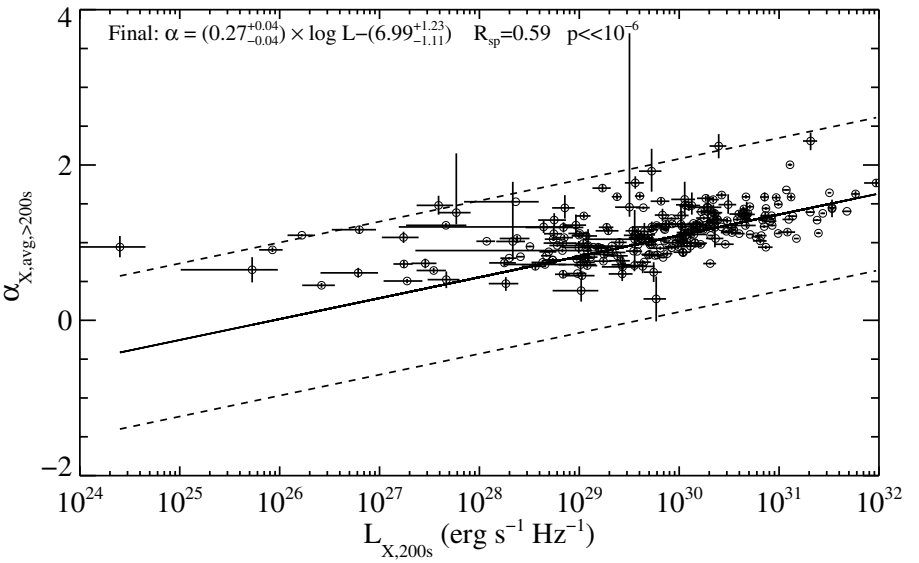

Fig. 1. Final average decay - luminosity correlation using the sample that includes flare correction and those only of long duration, with corrections and sub-sample optimisation described in §3. The solid line indicates the best fit regression, and the dashed lines indicates the 2σ deviation. This figure is reproduced from Fig. 9 of Ref. 12.

Table 2. For each pair of parameters examined, this table contains: the Spearman rank correlation coefficient with its associated null hypothesis; the coefficient of the partial Spearman rank with its associated null hypothesis; the slope and constant values provided by the best fit linear regression. We also provide the 1σ error of the Spearman rank coefficient. Table is a reproduction of Table 2 from Ref. 13.

Parameters		Spearman Rank	Null	Partial	Null	—Best fit linear regression—	
x-axis	y-axis	Coefficient	Hypothesis	Spearman Rank	Hypothesis	Slope	Constant
log $L_{O,200s}$	log $L_{X,200s}$	0.81 (0.05)	5.26×10^{-12}	0.70	2.85×10^{-8}	0.91 ± 0.22	1.04 ± 6.94
$\alpha_{O,>200s}$	$\alpha_{X,>200s}$	0.77 (0.07)	1.10×10^{-10}	0.75	1.27×10^{-9}	0.97 ± 0.10	0.25 ± 0.09
log $L_{O,200s}$	$\alpha_{O,>200s}$	0.58 (0.11)	1.90×10^{-5}	0.50	2.85×10^{-4}	0.28 ± 0.04	-7.72 ± 1.31
log $L_{X,200s}$	$\alpha_{X,>200s}$	0.69 (0.09)	8.03×10^{-8}	0.63	1.58×10^{-6}	0.26 ± 0.05	-6.71 ± 1.39
log $L_{O,200s}$	$\alpha_{X,>200s}$	0.60 (0.12)	6.87×10^{-6}	0.52	1.53×10^{-4}	0.29 ± 0.03	-8.13 ± 1.08
log $L_{X,200s}$	$\alpha_{O,>200s}$	0.65 (0.10)	5.58×10^{-7}	0.60	7.58×10^{-6}	0.32 ± 0.06	-8.70 ± 1.68
log E_{iso}	$\alpha_{O,>200s}$	0.54 (0.12)	9.05×10^{-5}	0.44	1.96×10^{-3}	0.21 ± 0.05	-10.22 ± 2.57
log E_{iso}	$\alpha_{X,>200s}$	0.57 (0.11)	3.12×10^{-5}	0.47	8.70×10^{-4}	0.21 ± 0.04	-9.60 ± 2.16
log E_{iso}	log $L_{O,200s}$	0.76 (0.06)	4.51×10^{-10}	0.66	4.59×10^{-7}	1.09 ± 0.13	-25.27 ± 6.92
log E_{iso}	log $L_{X,200s}$	0.83 (0.05)	5.04×10^{-13}	0.76	4.78×10^{-10}	1.10 ± 0.15	-27.81 ± 7.89
log E_{peak}	$\alpha_{O,>200s}$	0.45 (0.13)	2.05×10^{-3}	0.38	1.20×10^{-2}	0.48 ± 0.17	-0.22 ± 0.41
log E_{peak}	$\alpha_{X,>200s}$	0.48 (0.13)	9.22×10^{-4}	0.40	7.52×10^{-3}	0.48 ± 0.15	0.03 ± 0.36
log E_{peak}	log $L_{O\times200s}$	0.66 (0.11)	1.16×10^{-6}	0.58	3.51×10^{-5}	2.97 ± 0.76	24.53 ± 1.95
log E_{peak}	log $L_{X,200s}$	0.75 (0.10)	4.74×10^{-9}	0.70	1.38×10^{-7}	2.97 ± 0.67	22.50 ± 1.73

with $\alpha_{O,>200s}$ and $\alpha_{X,>200s}$. The Spearman rank coefficients are smaller than those found between luminosity and log E_{iso}, but do still indicate a correlation. Within 1σ the slopes of the linear regression for both the optical/UV and X-ray $\alpha_{>200s}$ versus log E_{iso} are consistent with each other. Similar results can are also found for

the four optical/UV and X-ray parameters versus E_{peak}, see Table 2. However, the relationships involving E_{peak} are weaker in comparison to the relationships observed with log E_{iso}; consistent with that found by Ref. 6.

4. Discussion

The log $L_{200s} - \alpha_{>200s}$ correlation, observed in the optical/UV and X-ray light curves, suggests that the brightest afterglows decay more quickly than the fainter afterglows. This points towards a common underlying mechanism producing the afterglow emission in the X-ray and optical/UV afterglows. We can therefore generally exclude models that invoke different emission mechanisms that would result in the log $L_{200s} - \alpha_{>200s}$ correlation being observed in only one frequency band.

Pre-*Swift* observations of late time X-ray afterglows also seemed to suggest the brightest X-ray afterglows decay more quickly than fainter afterglows,[22–24] but a larger sample including some of the first *Swift* X-ray light curves[25] was not able to support previous claims (see also Ref. 12). In this analysis, the correlation between luminosity and temporal behaviour is investigated at a much earlier time, when there is greater spread in the luminosity distribution, and the average decay index is determined using almost the entire observed afterglow.

We also have shown that the X-ray and optical/UV log L_{200s} are correlated with log E_{iso} and E_{peak}. This is consistent with previous studies (e.g. Refs. 23, 26–28), in particular Refs. 6 and 29, who performed a similar study using early X-ray luminosity, 5−10 minutes after trigger. We have also shown that the optical/UV and X-ray $\alpha_{>200s}$ are correlated with log E_{iso} and E_{peak}. Altogether, these correlations indicate that the GRBs with the brightest, fastest, decaying afterglows also have the largest observed prompt emission energies and typically larger peak spectral energy.

We now investigate if these observations are consistent with the predictions of a basic standard afterglow model; an isotropic outflow with no reverse shock or energy injection. The standard afterglow model predicts different relationships between L, α and other parameters depending on the location and ordering of the synchrotron spectral frequencies relative to the observing bands. Therefore to obtain the expected relationships between various parameters for a sample of GRBs we performed a Monte Carlo simulation. Using 10^4 trials, we simulated the optical/UV (at 1600 Å) and X-ray (at 1 keV) flux densities for 48 GRBs using equation 8 of Ref. 30 and equations 4, 5 and 6 given in Ref. 31 for $F_{\nu,max}$, ν_m and ν_c. In this simulation we assume that all GRBs are produced in a constant density medium. To compute $F_{\nu,max}$, ν_m and ν_c we needed to determine values for the microphysical parameters. These were selected at random from log-normal distributions which had 3σ intervals ranging between: 0.01-0.3 for the fraction of energy given to the electrons, ϵ_e; $5\times10^{-4}-0.5$ for the fraction of energy given to the magnetic field, ϵ_B, and $10^{-3}-10^{3}\mathrm{cm}^{-2}$ for the density of the external medium. For the electron energy index p, we centred the distribution at 2.4, as determined by Ref. 32, however, we set

the 1σ width to be 0.2 rather than 0.59. Since the closure relations fail for p values < 2, we re-selected p when $p < 2$ was selected. The value of p along with the position of ν_c relative to the observed band and redshift (selected from a uniform distribution with the range 0.5 - 4.5, a similar range as the observed sample) dictate the values of α, β and the k-correction (as given in Ref. 33).

For the 48 GRBs in each trial, we selected a prompt emission energy from a log-normal distribution with a 3σ range $10^{51} - 10^{54}$ erg; a range similar to that of the GRBs in this sample. We picked a random value between 10% and 99% for the efficiency, which we used to convert the prompt emission energy into kinetic energy. Once all the microphysical parameters, redshift and kinetic energy had been selected, we were then able to determine the position of ν_c and thus knew where it was in relation to ν_O and ν_X. With this information, we then calculated the value of the optical/UV and X-ray fluxes and converted these to luminosity. As a byproduct of calculating the optical/UV and X-ray luminosities, we also have simulated distributions for E_{iso} and α. Therefore we also produce predictions for comparisons that involve these parameters. For the parameters of 48 GRBs in each trial, we performed linear regression using the IDL routine *sixlin*, and we also calculated the Spearman rank coefficient. The results of the simulation can be found in Table 3.

Table 3. The Spearman rank coefficient and linear regression parameters as predicted by the synchrotron model for a sample of 48 GRBs. These values were computed with a Monte Carlo simulation with 10^4 trials. Table is a reproduction of Table 1 from Ref. 13.

Parameters		Simulated Spearman	—Best fit linear regression for simulation—	
x-axis	y-axis	Rank Coefficient	Slope	Constant
$\log L_{O,200s}$	$\log L_{X,200s}$	0.92 ± 0.0	0.82 ± 0.0	3.76 ± 1.25
$\alpha_{O,>200s}$	$\alpha_{X,>200s}$	0.74 ± 0.0	1.10 ± 0.1	0.04 ± 0.17
$\log L_{O,200s}$	$\alpha_{O,>200s}$	0.30 ± 0.14	0.04 ± 0.02	-0.31 ± 0.65
$\log L_{X,200s}$	$\alpha_{X,>200s}$	0.20 ± 0.14	0.04 ± 0.03	0.10 ± 0.78
$\log E_{iso}$	$\alpha_{O,>200s}$	0.06 ± 0.15	0.03 ± 0.06	-0.32 ± 2.91
$\log E_{iso}$	$\alpha_{X,>200s}$	0.09 ± 0.15	0.04 ± 0.06	-0.76 ± 3.13
$\log E_{iso}$	$\log L_{O,200s}$	0.51 ± 0.11	4.43 ± 1.03	-200.76 ± 54.10
$\log E_{iso}$	$\log L_{X,200s}$	0.54 ± 0.11	3.28 ± 0.71	-142.22 ± 37.33

In the basic standard afterglow model, the optical/UV and X-ray emission is produced by the same mechanism in an isotropic outflow, we would therefore expect to see relationships between $\log L_{O,200s}$ & $\log L_{X,200s}$ and $\alpha_{O,>200s}$ versus $\alpha_{X,>200s}$. Our observed relationships between these parameters can therefore be explained easily by the standard afterglow model and are fully consistent with the simulations. A relationship between $\log E_{iso}$ and $\log L_{200s}$ is also expected in the standard afterglow model, but the comparison of our observed relationship to the simulations suggests that the observed linear regression slope is less steep than predicted by the simulation. Furthermore, the relationships we observe, between $\log L_{200s}$ and $\alpha_{>200s}$,

and log E_{iso} and $\alpha_{>200s}$, are not expected in the standard afterglow model and are not predicted by the simulations.

Since the standard afterglow does not succeed in fully predicting all of our observed correlations, it is likely that a more complex outflow model is required. This conclusion is similar to that drawn during the separate investigation of the optical/UV log $L_{200s} - \alpha_{>200s}$ decay correlation.[11]

4.1. *Alternative Models*

There are three main possibilities that could make the outflow complex enough to be able to reproduce the observed correlations. The first is that perhaps there is some mechanism or parameter that controls the amount of energy given to and distributed during the prompt and afterglow phases and that also regulates the afterglow decay rate. This should occur in such a way that for events with the largest gamma-ray isotropic energy, the energy given to the afterglow is released quickly, resulting in an initially bright afterglow which decays rapidly. Conversely, if the gamma-ray isotropic energy is smaller, then the afterglow energy is released slowly over a longer period, the afterglow will be less bright initially and decay at a slower rate.

The second possibility is that the correlations could be a geometric effect, perhaps the result of the observer's viewing angle. Jets viewed away from the jet-axis may have fainter afterglows that decay less quickly in comparison to afterglows

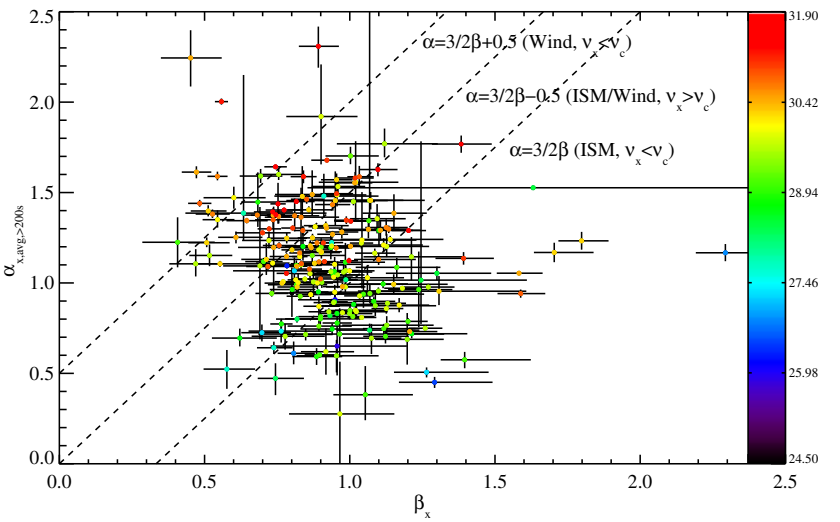

Fig. 2. The average temporal decay ($\alpha_{X,>200s}$) and average spectral energy index (β_X) are compared with $\log L_{X,200s}$ (colour scale), demonstrating consistency and trends with the closure relations (dashed lines). The high luminosity (redder) points are roughly consistent with wind-like environments. This figure is reproduced from Fig. 15 of Ref. 12.

viewed closer to the centre of the jet (see Fig 3. of Ref. 4). Similarly, this will also affect the observed prompt emission, with jets viewed off-axis appearing to have lower isotropic energy and lower peak spectral energy.[34]

The third possibility could be related to the circumburst environment. The closure relations relate α and the spectral index β through different relationships depending on the ordering of the synchrotron spectral parameters and the density profile or the external medium. If the correlation is affected by the circumburst environment, we expect to see GRBs with the highest luminosities favouring a particular environment. No apparent correlation is observed in the optical/UV.[11] However in the X-ray (see Figure 2), the highest luminosity GRBs tend toward the lines demarcating the r^{-2} wind environment. The ambiguity in the $\nu_x > \nu_c$ cases prohibits us from making a strong statement on the role of circumburst environment, but it may be another possible contribution in that the initially brightest GRB afterglows may be more likely to live in wind-like environments (see also Ref. 35).

5. Conclusions

This proceeding has summarised the work presented in Refs. 12 and 13. We have shown that the correlation between luminosity (measured at restframe 200 s; log L_{200s}) and average decay rate (measured from 200 s; $\alpha_{>200s}$) is observed in the X-ray light curve sample as well as the optical/UV.[11] When we rerun the correlations with the GRBs that overlap the optical/UV and X-ray samples we find the luminosity-decay correlations are consistent. This suggests a single underlying mechanism producing the correlations in both bands and it is not dependent on their detailed temporal behaviour. We also show significant correlations between the logarithmic optical/UV and X-ray luminosity (log $L_{O,200s}$, log $L_{X,200s}$) and the optical/UV and X-ray decay indices ($\alpha_{O,>200s}$ and $\alpha_{X,>200s}$) and all four of these parameters are found to be correlated with the prompt emission parameters: isotropic energy (E_{iso}) and restframe peak spectral energy (E_{peak}). Together these correlations imply that the GRBs with the brightest afterglows in the X-ray and optical/UV bands, decay the fastest and they also have the largest observed prompt emission energies and typically larger peak spectral energy. This suggests that what happens during the prompt phase has direct implications on the afterglow.

We used a Monte Carlo simulation to examine whether the standard afterglow model is able to explain the observed correlations. Overall, observed correlations between the luminosities in both the X-ray and optical/UV bands and between the luminosities and the isotropic energy are consistent with the predictions of the simulation. However, observed relationships involving the average decay indices with either luminosity at 200 s or the isotropic γ-ray energy are not consistent with the simulation. We therefore suggest that a more complex afterglow or outflow model is required to produce all the observed correlations. This may be due to either a viewing angle effect or by some mechanism or physical property controlling the

energy release within the outflow. The environment in which the GRB exploded may also contribute to the observed correlation.

Acknowledgements

This research has made use of data obtained from the High Energy Astrophysics Science Archive Research Center (HEASARC) and the UK Swift Science Data Centre provided by NASA's Goddard Space Flight Center and the University of Leicester, UK, respectively. MJP, AAB, NPMK and PJS acknowledge the support of the UK Space Agency.

References

1. L. Amati, F. Frontera, M. Tavani, J. J. M. in't Zand, A. Antonelli, E. Costa, M. Feroci, C. Guidorzi, J. Heise, N. Masetti, E. Montanari, L. Nicastro, E. Palazzi, E. Pian, L. Piro and P. Soffitta, Intrinsic spectra and energetics of BeppoSAX Gamma-Ray Bursts with known redshifts, *Astron. Astrophys.* **390**, 81 (July 2002).
2. G. Ghirlanda, G. Ghisellini and D. Lazzati, The Collimation-corrected Gamma-Ray Burst Energies Correlate with the Peak Energy of Their νF_ν Spectrum, *Astrophys. J.* **616**, 331 (November 2004).
3. M. G. Dainotti, V. F. Cardone and S. Capozziello, A time-luminosity correlation for γ-ray bursts in the X-rays, *Mon. Not. R. Astr. Soc.* **391**, L79 (November 2008).
4. A. Panaitescu and W. T. Vestrand, Taxonomy of gamma-ray burst optical light curves: Identification of a salient class of early afterglows, *Mon. Not. R. Astr. Soc.* **387**, 497 (June 2008).
5. M. G. Bernardini, R. Margutti, J. Mao, E. Zaninoni and G. Chincarini, The X-ray light curve of gamma-ray bursts: Clues to the central engine, *Astron. Astrophys.* **539**, p. A3 (March 2012).
6. P. D'Avanzo, R. Salvaterra, B. Sbarufatti, L. Nava, A. Melandri, M. G. Bernardini, S. Campana, S. Covino, D. Fugazza, G. Ghirlanda, G. Ghisellini, V. La Parola, M. Perri, S. D. Vergani and G. Tagliaferri, A complete sample of bright Swift Gamma-ray bursts: X-ray afterglow luminosity and its correlation with the prompt emission, *Mon. Not. R. Astr. Soc.* **425**, 506 (September 2012).
7. L. Li, E.-W. Liang, Q.-W. Tang, J.-M. Chen, S.-Q. Xi, H.-J. Lü, H. Gao, B. Zhang, J. Zhang, S.-X. Yi, R.-J. Lu, L.-Z. Lü and J.-Y. Wei, A Comprehensive Study of Gamma-Ray Burst Optical Emission. I. Flares and Early Shallow-decay Component, *Astrophys. J.* **758**, p. 27 (October 2012).
8. E.-W. Liang, L. Li, H. Gao, B. Zhang, Y.-F. Liang, X.-F. Wu, S.-X. Yi, Z.-G. Dai, Q.-W. Tang, J.-M. Chen, H.-J. Lü, J. Zhang, R.-J. Lu, L.-Z. Lü and J.-Y. Wei, A Comprehensive Study of Gamma-Ray Burst Optical Emission. II. Afterglow Onset and Late Re-brightening Components, *Astrophys. J.* **774**, p. 13 (September 2013).
9. E. Zaninoni, M. G. Bernardini, R. Margutti, S. Oates and G. Chincarini, Gamma-ray burst optical light-curve zoo: Comparison with X-ray observations, *Astron. Astrophys.* **557**, p. A12 (September 2013).
10. A. Panaitescu, W. T. Vestrand and P. Woźniak, Peaks of optical and X-ray afterglow light curves, *Mon. Not. R. Astr. Soc.* **433**, 759 (July 2013).
11. S. R. Oates, M. J. Page, M. De Pasquale, P. Schady, A. A. Breeveld, S. T. Holland, N. P. M. Kuin and F. E. Marshall, A correlation between the intrinsic brightness and

average decay rate of Swift/UVOT gamma-ray burst optical/ultraviolet light curves, *Mon. Not. R. Astr. Soc.* **426**, L86 (October 2012).

12. J. L. Racusin, S. R. Oates, M. de Pasquale and D. Kocevski, A Correlation between the Intrinsic Brightness and Average Decay Rate of Gamma-Ray Burst X-Ray Afterglow Light Curves, *Astrophys. J.* **826**, p. 45 (July 2016).
13. S. R. Oates, J. L. Racusin, M. De Pasquale, M. J. Page, A. J. Castro-Tirado, J. Gorosabel, P. J. Smith, A. A. Breeveld and N. P. M. Kuin, Exploring the canonical behaviour of long gamma-ray bursts using an intrinsic multiwavelength afterglow correlation, *Mon. Not. R. Astr. Soc.* **453**, 4121 (November 2015).
14. D. N. Burrows, J. E. Hill, J. A. Nousek, J. A. Kennea, A. Wells, J. P. Osborne, A. F. Abbey, A. Beardmore, K. Mukerjee, A. D. T. Short, G. Chincarini, S. Campana, O. Citterio, A. Moretti, C. Pagani, G. Tagliaferri, P. Giommi, M. Capalbi, F. Tamburelli, L. Angelini, G. Cusumano, H. W. Bräuninger, W. Burkert and G. D. Hartner, The Swift X-Ray Telescope, *Space Science Reviews* **120**, 165 (October 2005).
15. P. A. Evans, A. P. Beardmore, K. L. Page, L. G. Tyler, J. P. Osborne, M. R. Goad, P. T. O'Brien, L. Vetere, J. Racusin, D. Morris, D. N. Burrows, M. Capalbi, M. Perri, N. Gehrels and P. Romano, An online repository of Swift/XRT light curves of γ-ray bursts, *Astron. Astrophys.* **469**, 379 (July 2007).
16. P. A. Evans, A. P. Beardmore, K. L. Page, J. P. Osborne, P. T. O'Brien, R. Willingale, R. L. C. Starling, D. N. Burrows, O. Godet, L. Vetere, J. Racusin, M. R. Goad, K. Wiersema, L. Angelini, M. Capalbi, G. Chincarini, N. Gehrels, J. A. Kennea, R. Margutti, D. C. Morris, C. J. Mountford, C. Pagani, M. Perri, P. Romano and N. Tanvir, Methods and results of an automatic analysis of a complete sample of Swift-XRT observations of GRBs, *Mon. Not. R. Astr. Soc.* **397**, 1177 (August 2009).
17. J. L. Racusin, E. W. Liang, D. N. Burrows, A. Falcone, T. Sakamoto, B. B. Zhang, B. Zhang, P. Evans and J. Osborne, Jet Breaks and Energetics of Swift Gamma-Ray Burst X-Ray Afterglows, *Astrophys. J.* **698**, 43 (June 2009).
18. B. Zhang, Y. Z. Fan, J. Dyks, S. Kobayashi, P. Mészáros, D. N. Burrows, J. A. Nousek and N. Gehrels, Physical Processes Shaping Gamma-Ray Burst X-Ray Afterglow Light Curves: Theoretical Implications from the Swift X-Ray Telescope Observations, *Astrophys. J.* **642**, 354 (May 2006).
19. D. Grupe, C. Gronwall, X. Wang, P. W. A. Roming, J. Cummings, B. Zhang, P. Mészáros, M. D. Trigo, P. T. O'Brien, K. L. Page, A. Beardmore, O. Godet, D. E. vanden Berk, P. J. Brown, S. Koch, D. Morris, M. Stroh, D. N. Burrows, J. A. Nousek, M. McMath Chester, S. Immler, V. Mangano, P. Romano, G. Chincarini, J. Osborne, T. Sakamoto and N. Gehrels, Swift and XMM-Newton Observations of the Extraordinary Gamma-Ray Burst 060729: More than 125 Days of X-Ray Afterglow, *Astrophys. J.* **662**, 443 (June 2007).
20. M. G. Dainotti, R. Willingale, S. Capozziello, V. Fabrizio Cardone and M. Ostrowski, Discovery of a Tight Correlation for Gamma-ray Burst Afterglows with "Canonical" Light Curves, *Astrophys. J. Letters* **722**, L215 (October 2010).
21. M. G. Dainotti, V. Petrosian, J. Singal and M. Ostrowski, Determination of the Intrinsic Luminosity Time Correlation in the X-Ray Afterglows of Gamma-Ray Bursts, *Astrophys. J.* **774**, p. 157 (September 2013).
22. M. Boër and B. Gendre, Evidences for two Gamma-Ray Burst afterglow emission regimes, *Astron. Astrophys.* **361**, L21 (September 2000).
23. C. Kouveliotou, S. E. Woosley, S. K. Patel, A. Levan, R. Blandford, E. Ramirez-Ruiz, R. A. M. J. Wijers, M. C. Weisskopf, A. Tennant, E. Pian and P. Giommi, Chandra Observations of the X-Ray Environs of SN 1998bw/GRB 980425, *Astrophys. J.* **608**, 872 (June 2004).

24. B. Gendre and M. Boër, Decay properties of the X-ray afterglows of gamma-ray bursts, *Astron. Astrophys.* **430**, 465 (February 2005).
25. B. Gendre, A. Galli and M. Boër, X-Ray Afterglow Light Curves: Toward A Standard Candle?, *Astrophys. J.* **683**, 620 (August 2008).
26. M. De Pasquale, L. Piro, B. Gendre, L. Amati, L. A. Antonelli, E. Costa, M. Feroci, F. Frontera, L. Nicastro, P. Soffitta and J. in't Zand, The BeppoSAX catalog of GRB X-ray afterglow observations, *Astron. Astrophys.* **455**, 813 (September 2006).
27. M. Nysewander, A. S. Fruchter and A. Pe'er, A Comparison of the Afterglows of Short- and Long-duration Gamma-ray Bursts, *Astrophys. J.* **701**, 824 (August 2009).
28. D. A. Kann, S. Klose, B. Zhang, D. Malesani, E. Nakar, A. Pozanenko, A. C. Wilson, N. R. Butler, P. Jakobsson, S. Schulze, M. Andreev, L. A. Antonelli, I. F. Bikmaev, V. Biryukov, M. Böttcher, R. A. Burenin, J. M. Castro Cerón, A. J. Castro-Tirado, G. Chincarini, B. E. Cobb, S. Covino, P. D'Avanzo, V. D'Elia, M. Della Valle, A. de Ugarte Postigo, Y. Efimov, P. Ferrero, D. Fugazza, J. P. U. Fynbo, M. Gålfalk, F. Grundahl, J. Gorosabel, S. Gupta, S. Guziy, B. Hafizov, J. Hjorth, K. Holhjem, M. Ibrahimov, M. Im, G. L. Israel, M. Jeĺinek, B. L. Jensen, R. Karimov, I. M. Khamitov, Ü. Kiziloğlu, E. Klunko, P. Kubánek, A. S. Kutyrev, P. Laursen, A. J. Levan, F. Mannucci, C. M. Martin, A. Mescheryakov, N. Mirabal, J. P. Norris, J.-E. Ovaldsen, D. Paraficz, E. Pavlenko, S. Piranomonte, A. Rossi, V. Rumyantsev, R. Salinas, A. Sergeev, D. Sharapov, J. Sollerman, B. Stecklum, L. Stella, G. Tagliaferri, N. R. Tanvir, J. Telting, V. Testa, A. C. Updike, A. Volnova, D. Watson, K. Wiersema and D. Xu, The Afterglows of Swift-era Gamma-ray Bursts. I. Comparing pre-Swift and Swift-era Long/Soft (Type II) GRB Optical Afterglows, *Astrophys. J.* **720**, 1513 (September 2010).
29. R. Margutti, E. Zaninoni, M. G. Bernardini, G. Chincarini, F. Pasotti, C. Guidorzi, L. Angelini, D. N. Burrows, M. Capalbi, P. A. Evans, N. Gehrels, J. Kennea, V. Mangano, A. Moretti, J. Nousek, J. P. Osborne, K. L. Page, M. Perri, J. Racusin, P. Romano, B. Sbarufatti, S. Stafford and M. Stamatikos, The prompt-afterglow connection in gamma-ray bursts: a comprehensive statistical analysis of Swift X-ray light curves, *Mon. Not. R. Astr. Soc.* **428**, 729 (January 2013).
30. R. Sari, T. Piran and R. Narayan, Spectra and Light Curves of Gamma-Ray Burst Afterglows, *Astrophys. J. Letters* **497**, L17 (April 1998).
31. B. Zhang, E. Liang, K. L. Page, D. Grupe, B.-B. Zhang, S. D. Barthelmy, D. N. Burrows, S. Campana, G. Chincarini, N. Gehrels, S. Kobayashi, P. Mészáros, A. Moretti, J. A. Nousek, P. T. O'Brien, J. P. Osborne, P. W. A. Roming, T. Sakamoto, P. Schady and R. Willingale, GRB Radiative Efficiencies Derived from the Swift Data: GRBs versus XRFs, Long versus Short, *Astrophys. J.* **655**, 989 (February 2007).
32. P. A. Curran, R. L. C. Starling, A. J. van der Horst and R. A. M. J. Wijers, Testing the blast wave model with Swift GRBs, *Mon. Not. R. Astr. Soc.* **395**, 580 (May 2009).
33. E. Berger, S. R. Kulkarni and D. A. Frail, A Standard Kinetic Energy Reservoir in Gamma-Ray Burst Afterglows, *Astrophys. J.* **590**, 379 (June 2003).
34. E. Ramirez-Ruiz, J. Granot, C. Kouveliotou, S. E. Woosley, S. K. Patel and P. A. Mazzali, An Off-Axis Model of GRB 031203, *Astrophys. J. Letters* **625**, L91 (June 2005).
35. M. De Pasquale, S. Schulze, D. A. Kann, S. Oates and B. Zhang, Physical properties of rapidly decaying Afterglows, in *EAS Publications Series*, eds. A. J. Castro-Tirado, J. Gorosabel and I. H. Park, EAS Publications Series, Vol. 61, July 2013.